Landsat-4 and Landsat-5 MSS Coherent Noise: Characterization and Removal

James C. Tilton, Brian L. Markham, and *William L. Alford**
NASA Goddard Space Flight Center, Greenbelt, MD 20771

ABSTRACT: Data from the Multispectral Scanners (MSSs) onboard the Landsat-4 and Landsat-5 satellites have been found by other researchers to be generally comparable to the data received from the earlier Landsat MSSs, with the exception of a coherent noise pattern evident in the Landsat-4 MSS imagery data. This noise pattern was also quite evident in the early Landsat-D' (prelaunch Landsat-5) test data. The addition of low-pass filters to the Landsat-D' MSS detector outputs substantially reduced the coherent noise measured in prelaunch test data and in in-flight data from Landsat-5. In this report we characterize the coherent noise magnitude at its apparent dominant image domain period in the range of 3.5 to 4.0 pixels/cycle for each detector, and note the efficacy of the noise reduction filters on the Landsat-D' MSS and the in-flight Landsat-5 MSS. We also describe a technique for resequencing Landsat MSS data into the time order sampled at the MSS instrument. Analyzing the resequenced data, we show that the coherent noise signals apparent in the image domain are actually aliases of a much higher frequency noise signal and its harmonics. We then describe a technique based on filtering resequenced MSS data which can be used to filter coherent noise from Landsat-4 MSS data with minimal adverse impact on the image data.

INTRODUCTION

The Landsat-4 and Landsat-5 satellites carry both the Thematic Mapper (TM) and Multispectral Scanner (MSS) remote sensing instruments. The MSS instrument is similar to MSS instruments carried by Landsat-1, Landsat-2, and Landsat-3. However, the addition of the Thematic Mapper instrument to Landsat-4 and Landsat-5 required several design changes in the MSS instruments carried on these satellites because of the lower orbit and new satellite platform dictated by the Thematic Mapper instrument. These design changes were made in part to make the Landsat-4 and Landsat-5 MSS data radiometrically and geometrically compatible with the MSS data from the earlier Landsat satellites.

In late 1981, the National Aeronautics and Space Administration (NASA) announced the Landsat-D Image Data Quality Analysis (LIDQA) Program. The majority of the studies coordinated under this program focus on the Thematic Mapper instrument. However, a few studies look at the MSS instrument. The bulk of the results from these MSS studies can be found in Volume I of *Landsat-4 Science Characterization Early Results* (Barker, 1985).

The MSS instruments onboard Landsats-1 through 5 are four-band instruments with six detec-

tors per band (Landsat-3 carried a fifth band in the far infrared, but it failed early in the active life of Landsat-3). The four bands carried by all MSS instruments are green (0.5–0.6 μm), red (0.6–0.7 μm), near-IR (0.7–0.8 μm) and near-IR (0.8–1.1 μm). The radiometric quality of Landsat-4 MSS data has been found to be generally comparable to that of the previous MSS instruments. Radiometric striping (detector-to-detector) in the Landsat-4 MSS data has been found to be actually less than that found in the previous sensors (Alford and Imhoff, 1985; Rice and Malila, 1985). However, a new radiometric artifact has been observed in Landsat-4 MSS data. This coherent noise effect has been noted by several researchers to have a predominate spatial frequency in the neighborhood of 3.6 pixels/cycle (Alford and Imhoff, 1985; Rice and Malila, 1985; Likens and Wrigley, 1985). The magnitude (zero to peak) of this particular noise component has been generally measured to be about 0.6 counts. Other lower magnitude peaks have been less consistently observed, namely at about 2 pixels/cycle and 4.6 pixels/cycle by Rice and Malila (1985), and at about 11 pixels/cycle by Likens and Wrigley (1985) and Alford and Imhoff (1985). These noise frequency peaks constructively interfere at certain points in the imagery to produce occasional noise peaks which are much larger than the 0.6 counts observed for the major coherent noise peak at 3.6 pixels/cycle.
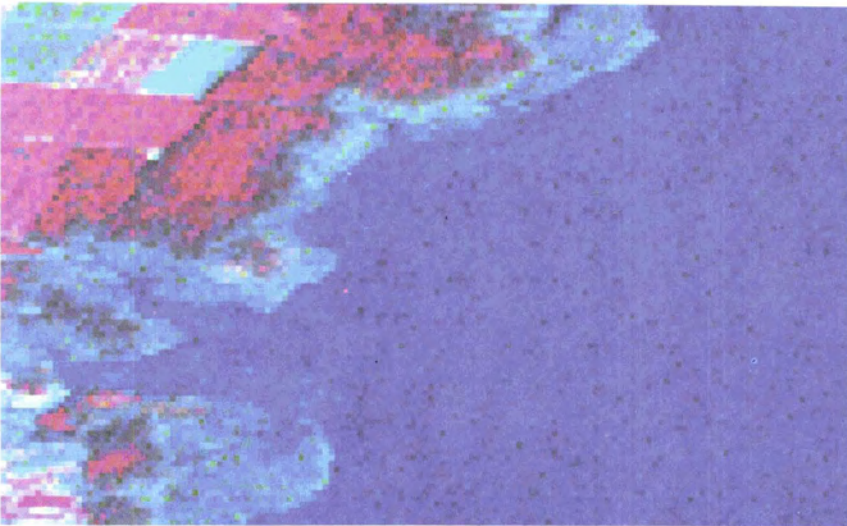
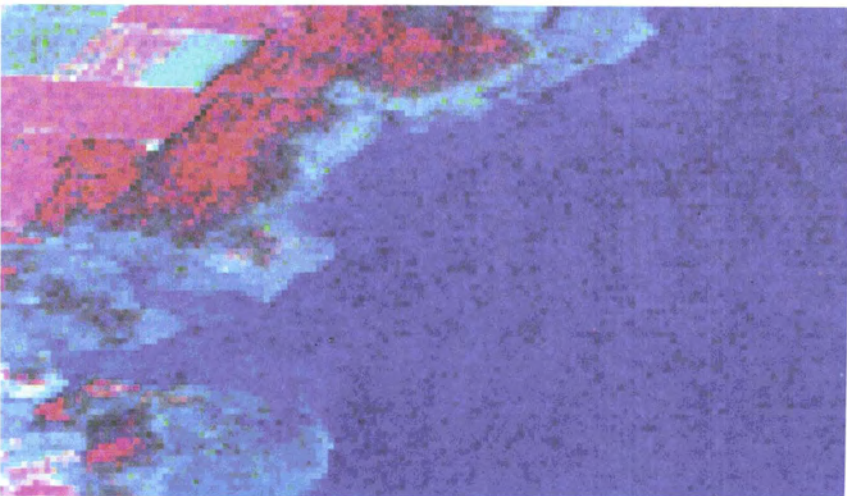A typical example of the coherent noise pattern is shown in Plate 1a. The structure of the noise pat-
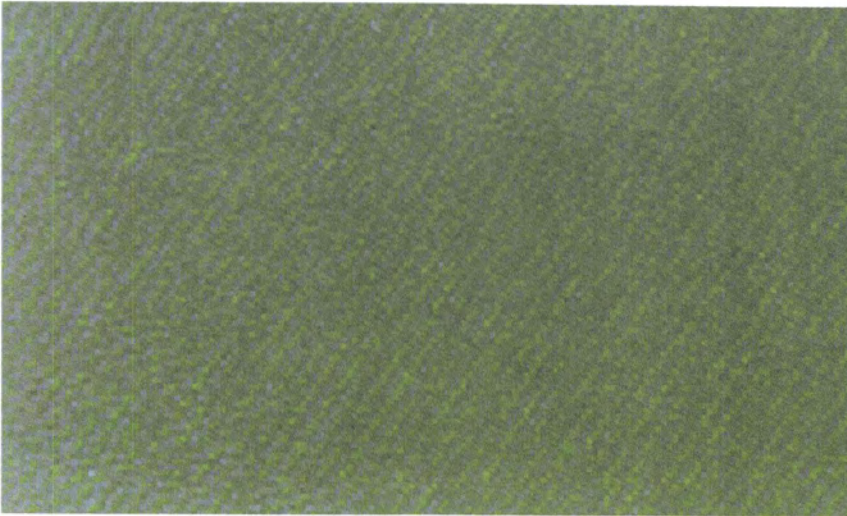
PLATE 1. (a) Original, (b) filtered and (c) difference image (plus bias) illustrating the Landsat-4 coherent noise problem. Shown is a 90 line by 157 column section of Landsat-4 MSS data (A-format CCT) over the coast of North Carolina obtained on 24 September 1982 (scene ID 84007015081, starting line 1801, starting column 2176).

tern can be seen more clearly by filtering out the noise pattern (using a technique developed in this paper) and displaying the difference image between the original and filtered images. Plate 1b is the filtered version of Plate 1a, and Plate 1c is the difference image. A constant bias was added to the difference image to produce a displayable positive image.

Plate 1c shows the coherent noise appears in the imagery as an oscillating noise pattern with a period of approximately 3 to 4 pixels running roughly diagonal from NNE to SSW. The oscillating noise pattern exhibits an irregular phase shift between groups of lines. This noise pattern can be detected most clearly in the original image over uniform areas such as bodies of water, and can be most easily seen if the image radiance values are stretched to fully utilize the dynamic range of the display device (as was done in Plate 1).

A comprehensive study of the effect of this noise pattern on the results obtained from various image analysis techniques has not been carried out. However, the noise pattern is apparently strong enough to affect analysis results. A rough idea of these effects can be obtained by clustering a section of original data, and comparing the resulting cluster map to one obtained by clustering a filtered version of the same section of data. We used the ISOCLAS function to cluster the original data shown in Plate 1a, and the filtered data shown in Plate 1b. We specified 16 clusters in both cases. Color coded maps of the resulting clusters are displayed in Plates 2a and 2b. The original data produce four water clusters, while the filtered data produce only one water cluster. The land clusters are also perturbed by the presence of the coherent noise.

We ran the ISOCLAS function with a set of parameters commonly used by analysts at NASA/GSFC for this type of data.* No attempt was made to adjust the parameters to minimize or maximize the unreasonable clusters caused by the noise in the data. Another clustering program, or ISOCLAS run with a different set of parameters might not produce such a pronounced effect from the noise. We know of at least one case where this noise effect has caused major problems for a research project. The noise effect causes classification errors between ocean and wetlands in a study of ocean instrusion over time along the Louisiana coast (Nelson May, personal communication, Center for Wetland Resources,

Louisiana State University, Baton Rouge, LA, 1984).

Given that the Landsat-4 MSS coherent noise can adversely affect analysis results, we should seek to characterize the noise more precisely and find a technique for filtering out the noise. We describe below such a characterization of the coherent noise, and follow the characterization with a description of a technique that filters out the noise while minimally affecting the image data itself.

The coherent noise pattern also appears in the original integrating sphere test data from the pre-flight Landsat-5 (Landsat-D') MSS instrument. The noise characterization we obtained here suggested that certain filters be added to the Landsat-D' MSS instrument. The integrating sphere test data show that the noise reduction filters do indeed eliminate a large part of the noise. Also, in-flight data from Landsat-5 confirms that the noise is substantially reduced. However, some coherent noise does remain. In addition to our discussion of characterization and removal of the more prominent Landsat-4 MSS coherent noise, we characterize the coherent noise remaining in the Landsat-5 MSS data, and evaluate the efficacy of the noise reduction filters added in the retrofit of the Landsat-D' (Landsat-5) MSS instrument.

BACKGROUND

LANDSAT MSS SAMPLING SCHEMA

The non-image domain noise characterization and filtering techniques investigated here are based on the manner in which the Landsat MSS systems gather image data. A simplified, but fairly complete description of this process is given by Gordon (1980). Further information particular to Landsat-4 and Landsat-5 can be found in NASA/GSFC (1984).

The Landsat MSS systems scan a six pixel swath each mirror forward scan. On an A-format CCT, lines 1 through 6 are from the first forward mirror scan, lines 7 through 12 are from the second forward scan, and lines $6n-5$ through $6n$ are from the nth forward scan. Since Landsat-4 and Landsat-5 are 4-band systems, 24 detectors are scanned in each forward scan.

Each detector is sampled in sequence. Let the four bands be designated by the numerals 1, 2, 3, and 4 and let the six rows in each scan be designated by the letters A, B, C, D, E, and F. With this coding, detector 1A corresponds to band 1, row 1; detector 2A corresponds to band 2, row 1; and detector 4F corresponds to band 4, row 6. The sampling sequence is: 1A, 2A, 1B, 2B, 1C, 2C, 1D, 2D, 1E, 2E, 1F, 2F, 3A, 4A, 3B, 4B, 3C, 4C, 3D, 4D, 3E, 4E, 3F, 4F. After the 24 detectors are sampled, a blank is inserted (this blank was reserved for the far-infrared band on Landsat-3), and the sampling sequence is repeated. The time spacing between each individual sample is 0.39832 microseconds,

---

* We ran the ISOCLAS function with ISTOP = 12, CHNTHS = 1.0, DLMIN = 1.0, STDMAX = 1.5, and MAXCLS = 16, where ISTOP is the maximum number of iterations, CHNTHS is the threshold for cluster chaining, any two clusters whose means are closer than DLMIN are combined, any cluster whose standard deviation is greater than STDMAX, and whose number of points is greater than 2(NMIN + 1) are split (where NMIN is the default 30 points), and MAXCLS is the maximum number of clusters.
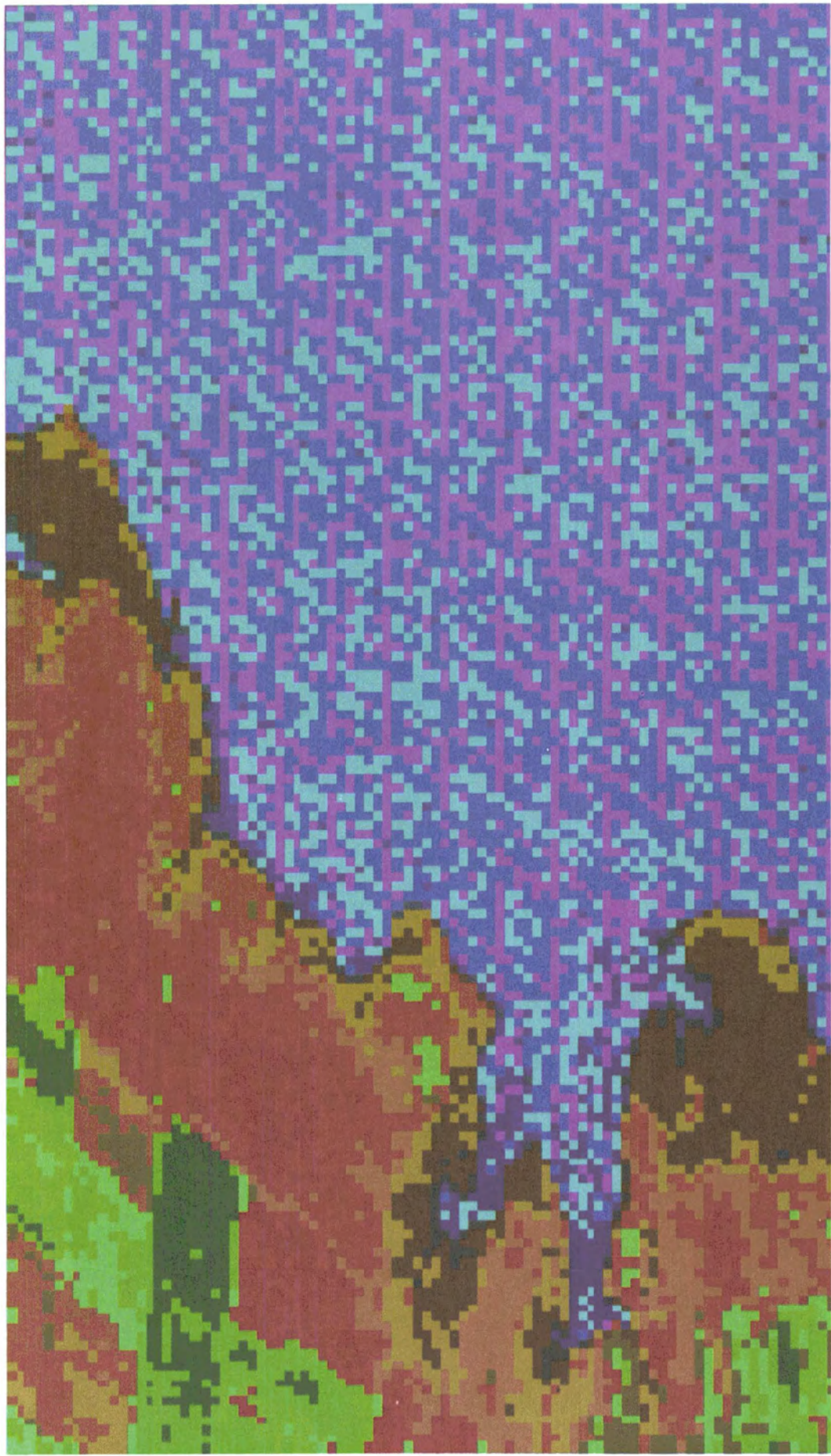
PLATE 2.   Cluster maps of a 90 line, 157 column portion of Landsat-4 MSS data over the coast of North Carolina obtained on 24 September 1982 (scene ID 84007015081, starting line 1801, starting column 2176). (a) original data. (b) filtered data.
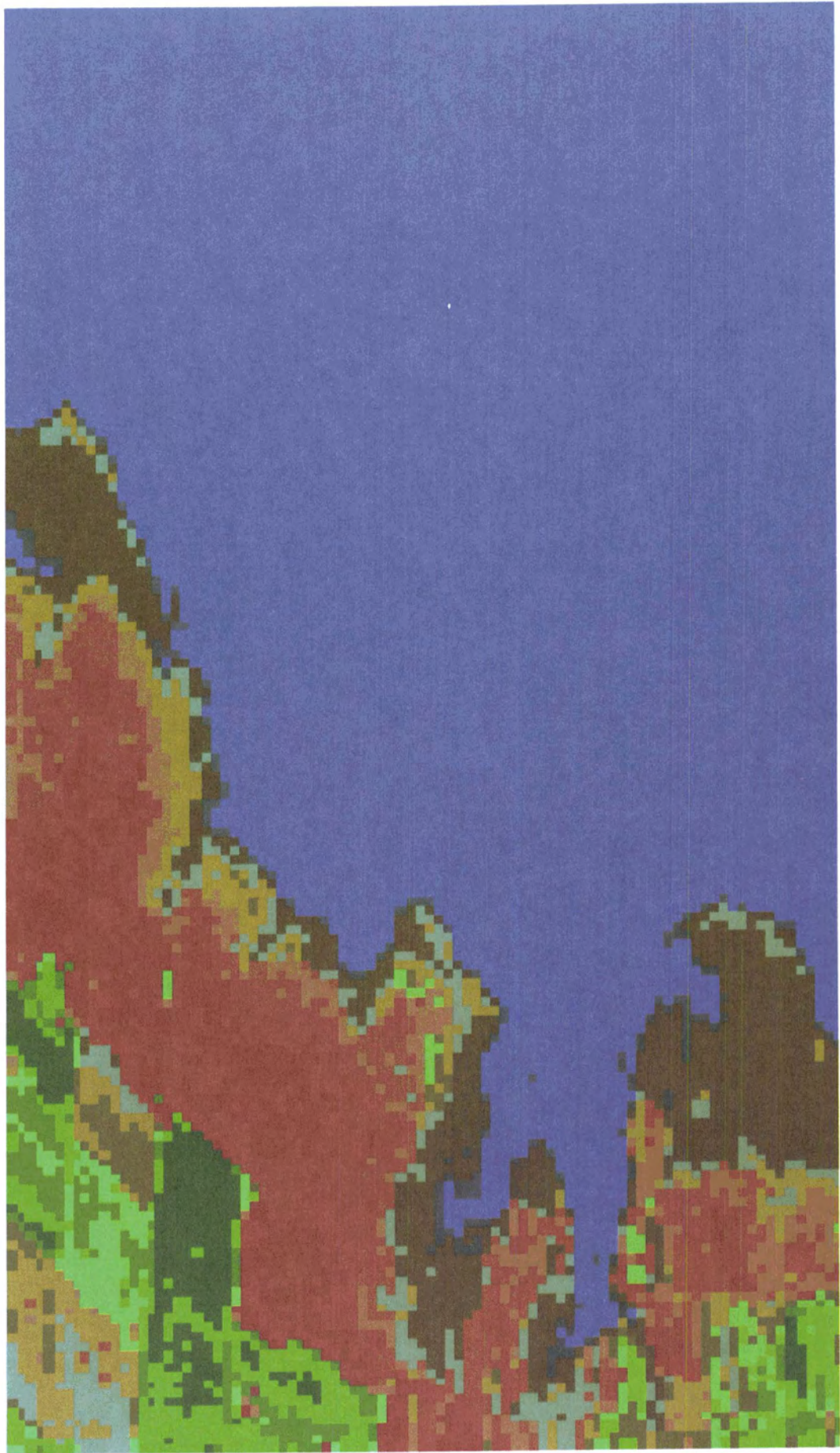
PLATE 2. Continued

and the entire sequence (including the blank) is re-sampled every 25 × 0.39832 or 9.958 microseconds.

Because of the physical layout of the detectors for each band of the MSS, the ground pixel locations of the four bands are offset from each other. If the MSS is scanning from west to east, in each sampling sequence the ground pixel location of band 2 is actually two pixels west of the ground pixel location of band 1, band 3 is four pixels west of band 1, and band 4 is six pixels west of band 1. This band-to-band offset is corrected for in A-format CCTs by the addition of six fill pixels to the start of each band 1 line, four fill pixels to the start and two fill pixels to the end of each band 2 line, two fill pixels to the start and four fill pixels to the end of each band 3 line, and six fill pixels to the end of each band 4 line.

IMPLICATIONS OF MSS SAMPLING SCHEMA

As mentioned above, Landsat-4 MSS image data exhibit an irregular oscillating noise pattern roughly 3 to 4 pixels in period. A 3 to 4 pixel period corresponds to a noise frequency range of 25 to 34 kHz. This frequency range corresponds to no candidate noise sources in the MSS electronics that are known to the authors. Image domain data is effectively sampled with a 9.958 microsecond sampling period; the period at which the entire 24 detector sequence is sampled. This sampling period corresponds to a sampling frequency of 100.42 kHz. With this sampling frequency, any noise frequency at over 50.2 kHz will appear at an alias frequency, and its true frequency could not be determined with any certainty. An analysis of the MSS data carried out directly in the image domain has little hope of pinning down the source of the noise if the noise has a frequency of over 50.2 kHz.

If the Landsat-4 MSS data were available in the original sampling sequence rather than image format, much higher frequency noise sources could be detected directly. As noted in the previous section, before the MSS data are put into image format, the data form a string of data points with a sampling period of 0.39832 microseconds which corresponds to a sampling frequency of 2510 kHz. If the blank sample after each group of 24 detector samples were filled in by interpolation, we could analyze the data as a string of samples taken at a sampling frequency 25 times that of the image domain sampling frequency. With a sampling frequency of 2510 kHz, we can directly determine the frequency of any noise frequency under 1255 kHz through the use of Fourier analysis. Since there are potential noise signals in the MSS electronics under 1255 kHz, we do have some hope of pinning down the source of the noise when we analyze the data in its original sampling sequence. In particular, one potential noise source is the power system with a nominal switching frequency of 110 kHz ± 5 kHz.

LANDSAT MSS DATA SOURCES

Landsat-4 or Landsat-5 MSS data are not available in the original sampling sequence. (Landsat-4 and Landsat-5 are referred to as Landsat-D and Landsat-D' prior to launch.) Landsat MSS digital image data sets are normally available in two formats: A-format CCT and P-format CCT. P-format data has undergone geometric resampling and is not appropriate for this study. A-format data has normally undergone radiometric correction though prior to launch; and as engineering data postlaunch, this data was often produced as raw data with unity-RLUTs, i.e., in the same format as A-data but with the radiometric lookup table (RLUT) generated from gains of one and offsets of zero.

The radiometric ground processing of MSS data can be thought of as occurring in two steps. First, the raw data from the sensor is decompressed (linearized) from 0-63 (6 bits) to 0-127 (7 bits). Bands 1–3 of MSS are normally acquired in a compressed mode, where the output is not a linear function of the input. The first step of the processing reverses this compression and expands band 4 linearly. The second step of the processing (the actual calibration step) adjusts each detector within a band to a common absolute radiometric range. Owing to the digital nature of the data and because both the decompression and calibration of the data are effectively expansions, certain count bins are empty in the calibrated data. These empty bins complicate the quantification of the magnitude of a low-level coherent noise effect. Thus, unity-RLUT or decalibrated data were used, as available, in determination of the magnitude of the coherent noise effects.

Decalibrated data can be generated from calibrated data using the gains and offsets provided on the CCTs, along with the decompression tables. Multiplying by the gain and adding the offset reverses the calibration. Then, using the decompression tables, the data can be mapped back to the raw data. Owing to the imprecision of the gains and offsets (e.g., offsets on tapes are quantized to 0.25 count), the data may be mapped to impossible count values, e.g., values not in the decompression table. The proper count can usually be determined and the data adjusted by examining the decompression table.

The data sets analyzed in this study are given in Table 1. The Integrating Sphere data sets are from unity-RLUT, A-format CCTs, and the other data sets from standard A-format CCTs.

NOISE ANALYSIS METHODS

MSS coherent noise analysis was carried out both in the image domain (directly from A-format CCTs), and in the original sampling domain. Analysis in the original sampling domain was conducted with re-sequenced data, i.e., A-format CCT data that was

TABLE 1. DATA SETS ANALYZED

Description	Date	Scene ID
Integrating Sphere (Landsat-D)	Sept. 10, 1981	—
Int. Sphere (Landsat-D' no filters)	Sept. 16, 1982	—
Int. Sphere (Landsat-D' with filters)	Sept. 29, 1983	32005-13380
Louisiana, Lake Pontchartrain (Landsat-4)	Sept. 16, 1982	84006215591
North Carolina, Atlantic Ocean (Landsat-4)	Sept. 24, 1982	84007015081
Florida, Gulf of Mexico (Landsat-4)	March 31, 1984	84062415465
Florida, Gulf of Mexico (Landsat-5)	April 24, 1984	85005415465

reformatted to the order in which it was originally sampled by the MSS instrument onboard Landsat-4 or Landsat-5.

IMAGE DOMAIN ANALYSES

Image domain analyses were conducted to characterize the coherent noise in Landsat-4 and Landsat-5 MSS data in the form normally available, viz, imagery. The magnitude and frequency of the noise effect by band and detector were characterized using uncalibrated (unity-RLUT), or decalibrated MSS data. Sixty line (10 swaths with 6 detectors/swath) by 512 pixel segments of data over areas apparently devoid of high frequency image content were selected for this study. Each detector's count values were normalized to mean zero by subtracting the appropriate offset. The magnitude of the Fourier transform of each detector line was calculated and the average over the 10 lines taken. Due to the discrete nature of the Fourier transform and the resulting dispersion of the noise peak between several adjacent values when the noise frequency is not exactly located at a sampled frequency, correction factors were calculated in order to determine the actual magnitude of the noise peak. For example, two equivalent noise peaks indicate (assuming only one really exists) that the true noise frequency occurs halfway between the two, with a magnitude 1.57 times either of the two. The magnitudes were interpolated at the nearest tenth of a cycle/512 pixels. The resulting numbers provided noise magnitudes (0-to-peak count) after nonlinear signal compression onboard the MSS. These

noise magnitudes would necessarily depend on the signal level. To remove this effect, the noise values were converted to equivalent linear (7 bit) count values using the decompression curve characteristics. A quadratic equation,

$$output = A*(input)^2 + B*(input) + C \quad (1)$$

was fitted to the decompression tables for Landsat-4 and Landsat-5 MSS data (Table 2) (NASA/GSFC, 1984). Bands 1 and 3 share a decompression table and band 4 is not compressed, so four equations resulted.

Thus, the magnitude of a noise peak in the raw data (MAG_{raw}) can be converted to a magnitude in decompressed data (MAG_{decom}) by:

$$MAG_{decom} = MAG_{raw}*GAIN \quad (2)$$

Where $GAIN = 2*A*Q + B$ where Q is the signal value in counts for the detector. These magnitudes are now comparable between dates and sensors. To convert the magnitudes to those that would be observed in the calibrated imagery, the gains on the A-tape $(GAIN_{cal})$ must be employed.

$$MAG_{cal} = MAG_{decom}/GAIN_{cal} \quad (3)$$

ANALYSES IN ORIGINAL SAMPLING SEQUENCE

Data from an A-format CCT can be put back into the order in which it was sampled at the MSS instrument. We call this reformatting process resequencing. Our resequencing process based on standard A-format CCT data does not recover the original data stream exactly because the A-format CCT data have been radiometrically decompressed and calibrated (as noted above). However, since the analysis in the original sampling sequence was conducted primarily to determine the frequency content of the data, rather than the magnitude of any particular frequency peak, we can use calibrated in-flight data from standard A-format CCTs in this analysis, without substantially affecting our results. Thus, we used standard A-format CCT data for analyzing in-flight data and uncalibrated raw data for analyzing prelaunch (Integrating Sphere) data.

The first step in resequencing is to take out the fill pixels (see Background section). Six pixels are deleted from the front of each line of band 1 (i.e., column 7 of band 1 becomes column 1), four pixels are deleted from the front of each line of band 2, and two pixels are deleted from the front of each line of band 3. Next, the data from each four band,

TABLE 2. FITTED DECOMPRESSION EQUATIONS

	Bands	A	B	C	R*R	SE	Gain (2AQ + B)
Landsat-4	1,3	0.02335	0.5475	0.7525	0.9997	0.6890	0.04670Q + 0.5475
Landsat-4	2	0.02349	0.5352	0.7870	0.9997	0.6507	0.04698Q + 0.5352
Landsat-5	1,3	0.02354	0.5312	0.8000	0.9998	0.5637	0.04708Q + 0.5312
Landsat-5	2	0.02364	0.5243	0.8775	0.9997	0.6754	0.04728Q + 0.5243

six line scan group is strung out according to the sampling sequence (see Background section) into one long data line. If an entire 2400 line, 3240 sample, four-band MSS scene is resequenced from an A-format CCT, the resulting data file would consist of 400 (2400/6) lines with 80,849 (25*(3240 − 6) − 1) samples in each line. As a part of the resequencing process, a value is interpolated for the blank sample period which occurs every $25n$ sample, $n = 1,2,\ldots,3233$. Thus, every $25n$ samples is the average of the $25n − 1$ sample and the $25n + 1$ sample.

Once a portion of the MSS data is resequenced, we can analyze it for possible noise frequencies. The most convenient way to do this is to take a one-dimensional Fourier transform of a piece of the data. Since the Fourier transform routine we utilized can handle a maximum of 4096 samples, we analyzed 6 line, 170 sample sections of the four-band MSS data, which when resequenced becomes 1 line by 4099 (25*(170-6)-1) samples. We take the Fourier transform of the first 4096 samples of this resequenced line of data.

One thing that we immediately noticed upon looking at a plot of the magnitude of the Fourier transform of resequenced data is that the amplitude of the frequency component corresponding to the sampling frequency of 100.42 kHz (period of 9.958 microseconds), and its harmonics, completely swamp out everything else. This is due to the differences in response across the four bands. In order to minimize the amplitude of these particular frequency components, we must add (subtract) a bias to (from) each of the bands so that all four bands have the same mean value before the resequencing and Fourier transform are performed. When this is done, the 100.42 kHz frequency and its harmonics are suppressed on a magnitude plot of the Fourier transform, and the frequency components corresponding to the coherent noise stand out distinctly.

NOISE CHARACTERIZATION RESULTS

IMAGE DOMAIN ANALYSIS RESULTS

Selected plots of the mean magnitudes of Fourier transforms of detector 1 for three scenes are presented in Figures 1 through 3. In all cases the 3.5–3.9 pixels/cycle noise peak dominated. The magnitudes of the peak are tabulated by band and detector in Tables 3 through 5. On Landsat-4, within a band, no consistent large differences were observed between detectors, with the possible exception of band 3 detector 6 having a lower magnitude than the rest of band 3. In terms of linearized noise counts (uncalibrated), band 1 averaged 0.52, band 2, 0.45, band 3, 0.40, and band 4, 0.36. Calibrated data noise magnitudes of 0.68, 0.69, 0.53, and 0.52 for bands 1 through 4, respectively, adjusted for ground processing changes as 0.70, 0.63, 0.58, and 0.45 compare favorably with magnitudes for these peaks of 0.75, 0.52, 0.56, and 0.50 reported by Rice and Malila (1985).

On Landsat-5, prior to installation of the noise

IMAGE DOMAIN FREQUENCY, PERIOD

FIG. 1. Fourier transform magnitude plot of a 512 sample segment of the Landsat-4 31 March 1984 scene of the Gulf of Mexico. Decalibrated data–detector 1 (band 1).

IMAGE DOMAIN FREQUENCY, PERIOD

FIG. 2. Fourier transform magnitude plot of a 512 sample segment of the Landsat-5 16 Sept. 1982 integrating sphere scene prior to filter installation. Uncalibrated data−detector 1 (band 1).
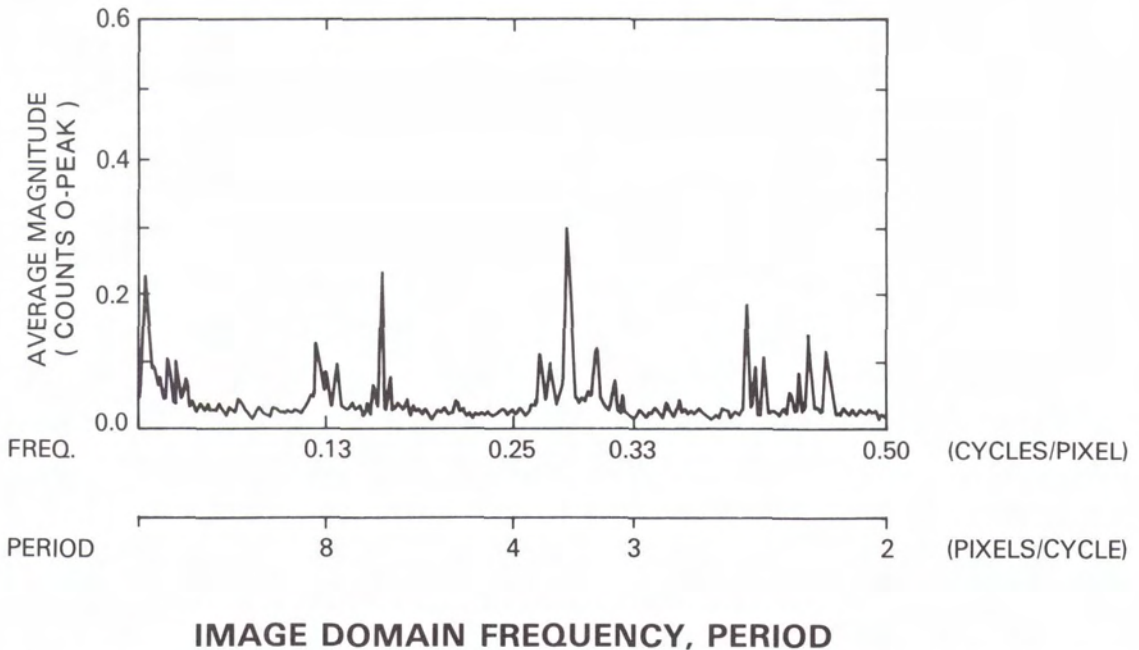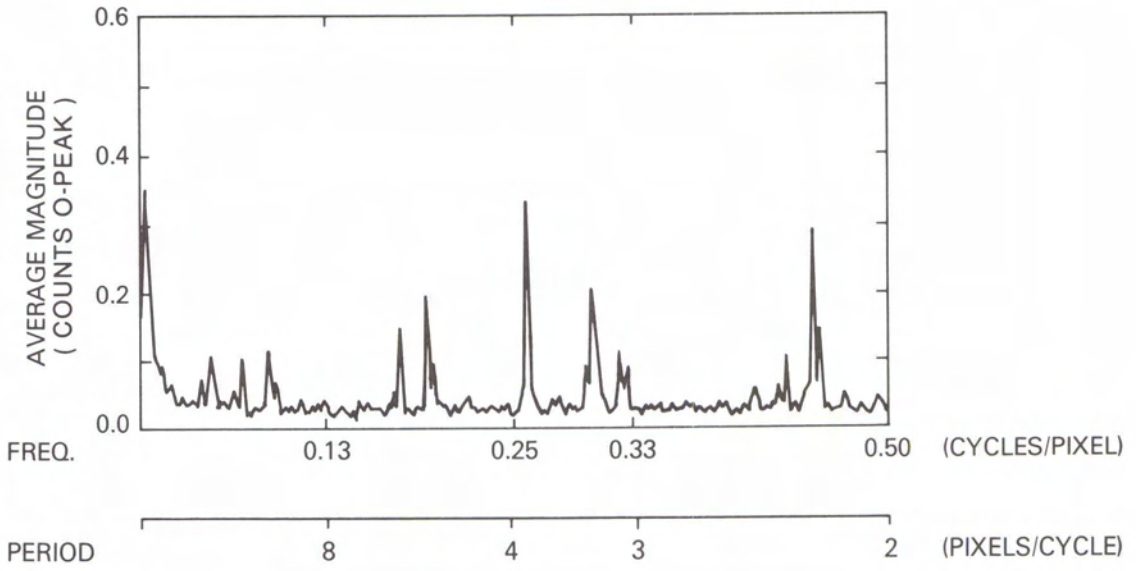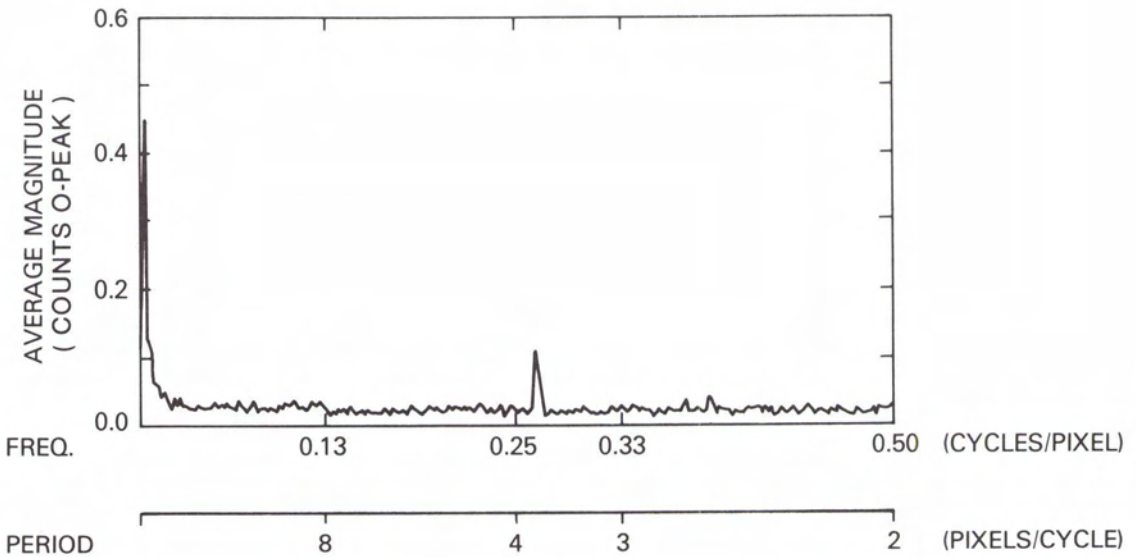

IMAGE DOMAIN FREQUENCY, PERIOD

FIG. 3. Fourier transform magnitude plot of a 512 sample segment of the Landsat-5 24 April 1984 scene of the Gulf of Mexico. Decalibrated data−detector 1 (band 1).

TABLE 3. LANDSAT-4 COHERENT NOISE MAGNITUDE 3.6 PIXELS/CYCLE PEAK (0-PEAK COUNTS) SAMPLE CALCULATIONS
31 MARCH 1984

DET	Peak Noise Magnitude	Interpolated Magnitude	Mean Signal Level (Counts)	Decompression Gain	Linearized Noise Magnitude	Calibration Gain	Calibrated Noise Magnitude
1	.30	.40	16.4	1.31	.52	1.235	.64
2	.34	.44	16.8	1.33	.59	1.198	.71
3	.28	.37	19.3	1.45	.53	1.035	.55
4	.30	.40	17.0	1.34	.54	1.178	.64
5	.32	.43	13.3	1.17	.51	1.590	.81
6	.32	.43	15.1	1.25	.53	1.316	.70
$\bar{x}$	.31	.41	—	—	.54	—	.68
	A	B ($A \times 1.32$)	C	D ($0.04670 \times C + 0.05475$)	E ($B \times D$)	F (from A-tape)	G ($E \times F$)

reduction filters, the noise levels were comparable, though averaging somewhat less than Landsat-4. Post filter installation, the magnitudes average approximately 60 percent less in bands 1–3, and 30 percent less in band 4. There is an indication that in band 4, the noise level increased since initial measurements after filter installation, with a net reduction of only 10 percent. Landsat-5 calibrated noise values showed magnitudes about 60 percent less than Landsat-4 in band 1, 70 percent less in band 2, 65 percent less in band 3, and 35 percent less in band 4.

RESULTS FROM ANALYSES IN ORIGINAL SAMPLING SEQUENCE

The noise frequency characterization studies were carried out on the Landsat-D (prelaunch Landsat-4) and Landsat-D' (prelaunch Landsat-5) MSS Integrating Sphere data, and on three Landsat-4 MSS scenes, and on one Landsat-5 MSS scene. The Landsat-D' data included data from before and after the installation of noise filters (see Table 1). The specific 6 line by 170 sample sections of these data sets used in the analysis are listed in Table 6.

TABLE 4. LANDSAT-4 COHERENT NOISE MEAN MAGNITUDE @ ~3.6 PIXELS/CYCLE PEAK (0-PEAK COUNTS)

DET #	Band 1 Linearized RAW IS-Prelaunch	Band 1 Linearized RAW 3/31/84	Band 1 Calibrated 3/31/84	Band 2 Linearized RAW IS-Prelaunch	Band 2 Linearized RAW 3/31/84	Band 2 Calibrated 3/31/84
1	0.47	0.52	0.64	0.45	0.50	0.85
2	0.54	0.59	0.71	0.54	0.48	0.63
3	0.49	0.53	0.55	0.36	0.48	0.69
4	0.48	0.54	0.64	0.43	0.46	0.76
5	0.48	0.51	0.81	0.43	0.45	0.59
6	0.50	0.53	0.70	0.45	0.41	0.61
$\bar{x}$	0.49	0.54	0.68	0.44	0.46	0.69

DET #	Band 3 Linearized RAW IS-Prelaunch	Band 3 Linearized RAW 3/31/84	Band 3 Calibrated 3/31/84	Band 4 Linearized RAW IS-Prelaunch	Band 4 Linearized RAW 3/31/84	Band 4 Calibrated 3/31/84
1	0.46	0.49	0.58	0.30	0.36	0.50
2	0.36	0.48	0.60	0.34	0.40	0.52
3	0.41	0.45	0.48	0.44	0.44	0.60
4	0.35	0.50	0.57	0.37	0.36	0.47
5	0.30	0.45	0.53	0.26	0.42	0.60
6	0.22	0.36	0.42	0.30	0.33	0.46
$\bar{x}$	0.35	0.46	0.53	0.33	0.39	0.52

TABLE 5.   LANDSAT-5 COHERENT NOISE MEAN MAGNITUDE @ ~3.9 PIXELS/CYCLE PEAK (0-PEAK COUNTS)

DET #	Band 1				Band 2			
	Linearized RAW			Calibrated	Linearized RAW			Calibrated
	IS-Pre-Fil	IS-Post-Fil	4/24/84	4/24/84	IS-Pre-Fil	IS-Post-Fil	4/24/84	4/24/84
1	0.40	0.13	0.19	0.23	0.37	0.16	0.18	0.23
2	0.40	0.11	0.17	0.21	0.37	0.12	0.17	0.23
3	0.41	0.12	0.22	0.28	0.38	0.12	0.14	0.19
4	0.39	0.14	0.18	0.27	0.38	0.13	0.18	0.25
5	0.39	0.15	0.18	0.33	0.36	0.13	0.15	0.20
6	0.38	0.14	0.22	0.39	0.29	0.14	0.14	0.18
$\bar{x}$	0.40	0.13	0.19	0.28	0.36	0.13	0.16	0.21

DET #	Band 3				Band 4			
	Linearized RAW			Calibrated	Linearized RAW			Calibrated
	IS-Pre-Fil	IS-Post-Fil	4/24/84	4/24/84	IS-Pre-Fil	IS-Post-Fil	4/24/84	4/24/84
1	0.44	0.15	0.12	0.15	0.37	0.16	0.24	0.32
2	0.40	0.14	0.13	0.16	0.31	0.14	0.29	0.39
3	0.38	0.16	0.19	0.22	0.31	0.13	0.30	0.41
4	0.38	0.13	0.13	0.14	0.23	0.19	0.22	0.30
5	0.40	0.13	0.18	0.24	0.33	0.20	0.21	0.28
6	0.30	0.13	0.14	0.16	0.21	0.14	0.30	0.41
$\bar{x}$	0.38	0.14	0.15	0.18	0.29	0.16	0.26	0.35

For each 6 line by 170 sample study site, separate biases were first added to (or subtracted from) each band to produce a mean value of 25 (after rounding) in each band. Then each study site was resequenced, and the magnitude of the Fourier transform of each resequenced data set was plotted.

As an example, Figure 4 shows the Fourier transform magnitude plot for the North Carolina study site. In the plot we notice some two or three dozen peaks. Even though the study site is over a very radiometrically flat area (the Atlantic Ocean), not all of the peaks are due to coherent noise. Some peaks are due to the residual differences between bands that remain even after the means of each band are

TABLE 6.   NOISE FREQUENCY CHARACTERIZATION STUDY SITES

Scene	Starting Line	Starting Pixel	Number of Lines	Number of Pixels
Integrating Sphere (D)	13	2101	6	170
Integrating Sphere (D)	1201	2101	6	170
Integrating Sphere (D)	2383	2101	6	170
Int. Sphere (D' no filters)	7	1621	6	170
Int. Sphere (D' with filters)	7	1621	6	170
Louisiana (4)	1423	1301	6	170
Louisiana (4)	1261	1781	6	170
North Carolina (4)	481	2001	6	170
Florida (4)	433	131	6	170
Florida (5)	433	11	6	170
Florida (5)	433	341	6	170

equalized. These residual differences result from several sources. As noted previously, variations have been observed in noise levels between detectors and bands. Also, detector-to-detector radiometric striping is present. As mentioned earlier, these resequencing artifact peaks occur at a frequency of 100.42 kHz (period of 9.958 microseconds), and at the harmonics of this frequency. To identify these artifact peaks clearly on our Fourier transform magnitude plots, we have plotted the magnitudes versus image domain frequency in cycles/pixel. In this scale, the artifact peaks occur at integer values (1, 2, 3, . . .). Note that 1 cycle/pixel in the image domain is equal to 1/25 cycle/sample or 100.42 kHz in the resequenced sampling domain.

The largest noise peak in the North Carolina study site Fourier transform plot (Figure 6) is at an image domain frequency of 2.28 cycles/pixel. This corresponds to a resequenced domain frequency of about 229 kHz. We note that this frequency is very near the second harmonic of the power system switching frequency of 110 kHz ± 5 kHz.

The Fourier transform plots for each study site contain several peaks attributable to the coherent noise. These peaks are very similar in amplitude and frequency across all study sites, and were constant in frequency across study sites within a particular data set. In each case the largest noise peak is very near the second harmonic of the power system switching frequency (see Table 7). This behavior is consistent with a hypothesis that the noise signal source is a slowly drifting oscillator, possibly in the
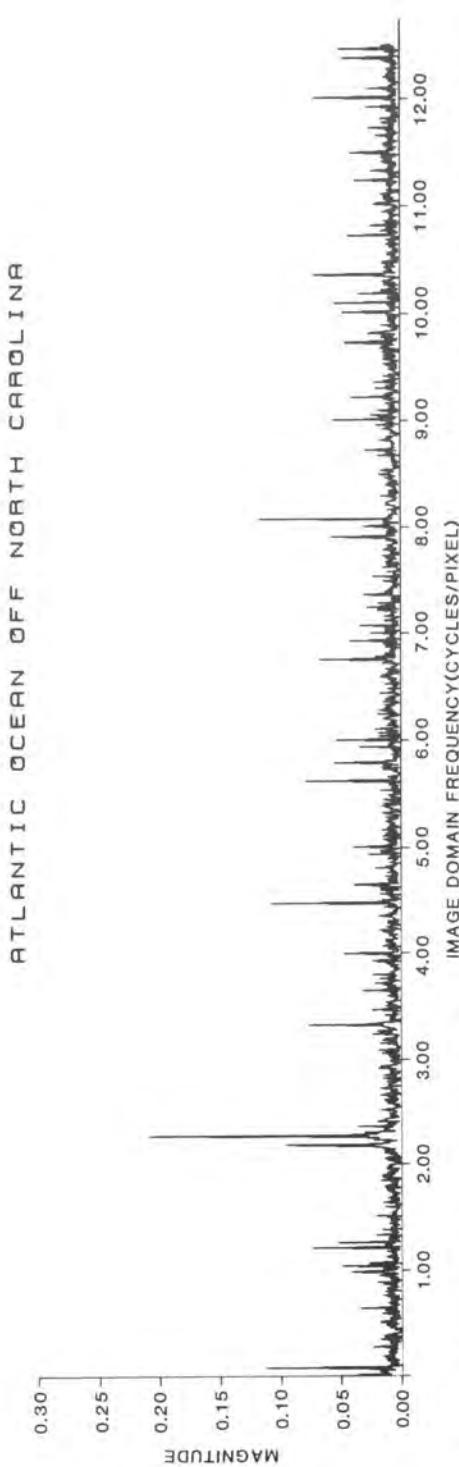
Fig. 4. Fourier transform magnitude plot of a 4096-sample resequenced sample of the North Carolina study site. The site is of the Atlantic Ocean off the North Carolina coast. (Only the positive, nonzero frequency components are displayed: calibrated data, magnitude in counts.)

TABLE 7. LARGEST COHERENT NOISE PEAKS. (POWER SYSTEM SWITCHING FREQUENCY IS 110 kHz ± 5 kHz)

Scene	Frequency (kHz)	Frequency/2 (kHz)*
Integrating Sphere (D)	228	114.0
Integrating Sphere (D')	226	113.0
Louisiana (4)	229	114.5
North Carolina (4)	229	114.5
Florida (4)	229	114.5
Florida (5)	227	113.5

* Values are rounded to the nearest 0.5 kHz.

DC to DC voltage converter or chopper voltage regulator.

We noted in the introduction that the coherent noise appears as an oscillating pattern approximately 3 to 4 pixels in period running roughly diagonal from NNE to SSW in the MSS imagery. Frequencies in the range of 226 to 230 kHz (2.25 to 2.29 cycles/pixel) will appear at an alias frequency of 25.1 to 29.1 kHz (0.25 to 0.29 cycles/pixel), or at a period of 3.4 to 4.0 pixels. This aliasing corresponds precisely to what we observe in the imagery.

A tabulation of the noise peaks for selected scenes are presented in Tables 8 through 10. For Landsat-5 (D') the reduction in the noise peaks upon addi-

TABLE 8. LANDSAT-4 NORTH CAROLINA DATA OBSERVED COHERENT NOISE FREQUENCY PEAKS

Frequency (cycles/ (4096 samples))	Frequency (cycles/ pixel)	Aliased Period in Image Domain (pixels)	Fourier Magnitude
14	0.09	11	0.11
173	1.06	17	0.05
201	1.23	4.3	0.07
210	1.28	3.6	0.05
360	2.20	5.0	0.10
374	2.28	3.6	0.21
388	2.37	2.7	0.04
546	3.33	3.0	0.08
733	4.47	2.1	0.11
761	4.64	2.8	0.04
920	5.62	2.6	0.08
948	5.79	4.8	0.06
1107	6.76	4.2	0.07
1135	6.93	14	0.04
1294	7.90	10	0.06
1322	8.07	14	0.12
1509	9.21	4.8	0.04
1592	9.72	3.6	0.05
1653	10.09	11	0.05
1667	10.17	5.9	0.04
1696	10.35	2.9	0.07
1756	10.72	3.6	0.04
1840	11.23	4.3	0.04
1882	11.49	2.0	0.04
2027	12.37	2.7	0.05
2041	12.46	2.2	0.05

TABLE 9. LANDSAT-D' INTEGRATING SPHERE OBSERVED COHERENT NOISE FREQUENCY PEAKS (WITHOUT RC FILTERS)

Frequency		Aliased Period in Image	
(cycles/ (4096 samples))	(cycles/ pixel)	Domain (pixels)	Fourier Magnitude
31	0.19	5.3	0.08
133	0.81	5.3	0.02
154	0.94	17	0.03
216	1.32	3.1	0.05
370	2.26	3.8	0.08
401	2.45	2.2	0.07
523	3.19	5.3	0.03
564	3.44	2.3	0.02
585	3.57	2.3	0.02
708	4.32	3.1	0.02
739	4.51	2.0	0.02
770	4.70	3.3	0.09
893	5.45	2.2	0.04
955	5.83	5.9	0.05
1078	6.58	2.4	0.03
1140	6.96	25	0.04
1324	8.08	12.5	0.03
1632	9.96	25	0.03

tion of the low pass filters is evident. The filtering design used was a single-pole RC filter (Peter Malherbe, General Electric Company, Valley Forge, PA, personal communication, 1984): $MTF = 1/(1 + (f/fc)^2)^{.5}$ with the cut-off frequency (fc) equal to 94.6 kHz for bands 1 through 3 and 141.8 kHz for band 4. With the knowledge that the image domain peak noise (at approximately 3.8 pixels or 30 kHz) is actually the alias of a 227 kHz signal, the noise reduction in the image domain is explainable. In bands 1 through 3, a 227 kHz noise should be reduced 62 percent by the specified filter; in band 4 the reduction should be 48 percent. These reductions are consistent with the reported approximate 60 percent reduction in bands 1 through 3 and 45 percent prelaunch for band 4 (previous section). However, postlaunch Landsat-5 data suggest the noise increased in band 4, with a net reduction of only 10 percent. If the filter is performing as specified, then most of the rest of the noise peaks, being higher frequencies, would be expected to be reduced to a greater extent. The plots indicate they have been (see Figures 5a and 5b), with most peaks being brought down to the level of the background

TABLE 10. LANDSAT-D' INTEGRATING SPHERE OBSERVED COHERENT NOISE FREQUENCY PEAKS (WITH RC FILTERS)

Frequency		Aliased Period in Image	
(cycles/ (4096 samples))	(cycles/ pixel)	Domain (pixels)	Fourier Magnitude
33	0.20	5.0	0.02
369	2.25	4.0	0.04
402	2.45	2.2	0.02
772	4.71	3.4	0.02

noise. Even the 0.190 cycles/pixel peak (19 kHz) is significantly reduced, whereas by the filter it should be reduced only 2 percent. One explanation is that this peak is actually an alias of an even higher frequency. We discuss this theory in the following section.

HARMONIC RELATIONSHIPS AMONG COHERENT NOISE COMPONENTS

A cursory look at Tables 8 through 10 may not reveal any relationship between the frequencies of the various coherent noise peaks. However, a closer look at the frequencies of the larger noise peaks reveals that, if sufficiently high harmonics are considered, almost all of the noise peaks are harmonically related to each other. To see this we must remember that harmonics at frequencies higher than the Nyquist frequency (in this case, 12.5 cycles/pixel) appear in the Fourier magnitude plots as alias frequencies. For example, the thirteenth harmonic of 1 cycle/pixel (13 cycles/pixel) would appear at 12 cycles/pixel (25 − 13 = 12), and the twenty-sixth harmonic (26 cycles/pixel) would appear at 1 cycle/pixel (26 − 25 = 1).

To see how this occurs in the Landsat MSS coherent noise data, consider the North Carolina data as an example. The largest peak in the North Carolina data set occurs at 2.28 cycles/pixel. We could take 2.28 cycles/pixel to be the fundamental frequency and look for harmonics of 2.28 cycles/pixel in the data. However, we will find that many more noise peaks can be harmonically related if we consider 1.14 cycles/pixel to be the fundamental frequency and 2.28 cycles/pixel to be the second harmonic of the fundamental frequency.

Considering the third through the tenth harmonic of 1.14 cycles/pixel, we do not find any corresponding noise peaks. The tenth harmonic (11.4 cycles/pixel) is also the highest harmonic we can directly observe in the Fourier transform magnitude plot. The eleventh harmonic is at 12.54 cycles/pixel, which is 0.04 cycles/pixel higher than the Nyquist frequency. Thus, if we have a noise peak at the eleventh harmonic, it would appear at 12.50 − 0.04 = 12.46 cycles/pixel in the Fourier magnitude plot. Looking back at Table 8, we see that we do indeed have a noise peak at 12.46 cycles/pixel. The twelfth harmonic at 13.68 cycles/pixel would appear as an alias frequency of (12.50 − (13.68 − 12.50)) = (25.00 − 13.68) = 11.32 cycles/pixel. We do not see a noise peak at 11.32 cycles/pixel in Table 8, but we do see a noise peak at the thirteenth harmonic (25.00 − 14.82 = 10.18 cycles/pixel), and at the fifteenth (7.90 cycles/pixel), sixteenth (6.76 cycles/pixel), seventeenth (5.62 cycles/pixel), eighteenth (4.48 cycles/pixel), nineteenth (3.34 cycles/pixel), twentieth (2.20 cycles/pixel), and twenty-first (1.06 cycles/pixel) harmonics.

The twenty-second harmonic at 25.08 cycles/pixel would appear at an alias frequency of 0.08 cycles/
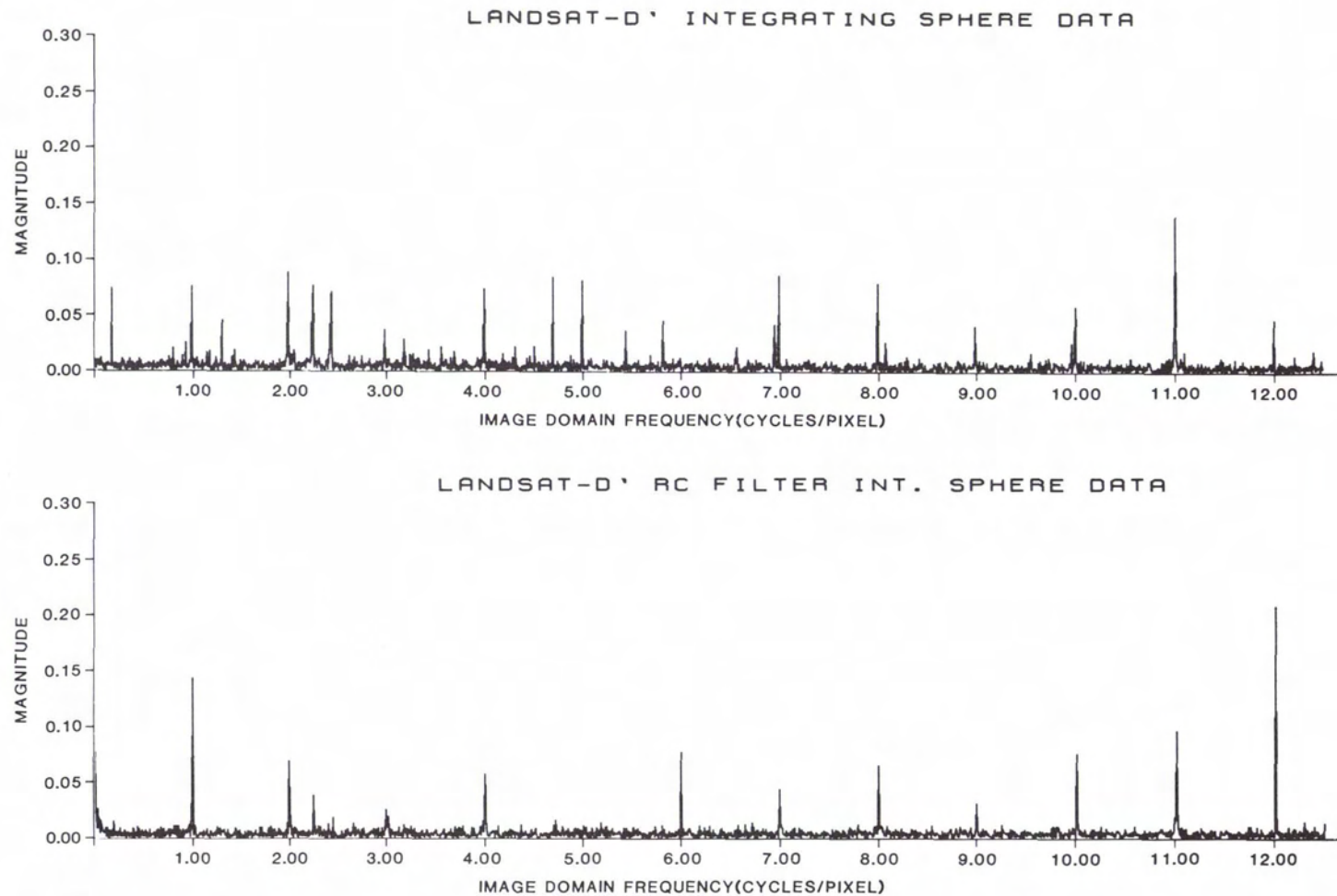
FIG. 5. Fourier transform magnitude plots of a 4096-sample resequenced sample of Integrating Sphere data from the (a) original and (b) filtered Landsat-D′ MSS instrument. (Only the positive, nonzero frequency components are displayed. Uncalibrated data, magnitude in counts.)

pixel (25.08 − 25.00). This is very close in frequency to the large peak at 0.09 cycles/pixel. Similarly we see noise peaks at the twenty-third harmonic (26.22 − 25.00 = 1.22 cycles/pixel), and the twenty-fourth (2.36 cycles/pixel), twenty-sixth (4.64 cycles/pixel), twenty-seventh (5.78 cycles/pixel), twenty-eighth (6.92 cycles/pixel), twenty-ninth (8.06 cycles/pixel), thirtieth (9.20 cycles/pixel), thirty-first (10.34 cycles/pixel), and thirty-second (11.48 cycles/pixel) harmonics.

The thirty-third harmonic is at 37.62 cycles/pixel, which would appear at an alias frequency of 12.38 cycles/pixel (50.00 − 37.62 = 12.38). This is very near the noise peak at 12.37 cycles/pixel. Similarly, we see noise peaks at the thirty-fourth harmonic (50.00 − 38.76 = 12.24 cycles/pixel), and at the thirty-fifth harmonic (10.10 cycles/pixel).

The only noise peaks that cannot be associated with harmonics of 35 or less of 1.14 cycles/pixel are the noise peaks at 1.28, 9.72, and 10.72 cycles/pixel. We see here that only 3 out of 26 noise peaks cannot be related to each other in this way. (These peaks could even be due to some other noise source.)

The harmonic relationships can be made even more exact if we take our fundamental frequency to be a best fit to all the inferred harmonics. The best fit fundamental frequency for the North Carolina data set is 1.1403 cycles/pixel.

Table 11 shows the inferred relationships among the noise peaks for the North Carolina data set. Similar results were found for all other data sets that we studied. The table lists the observed frequency, the inferred harmonic number, and the inferred frequency each observed frequency is an alias of, if it is indeed the inferred harmonic of the fundamental. The best fit fundamental frequency is given in a footnote to the table. In addition, the table lists the harmonic frequencies calculated by multiplying the harmonic number times the best fit fundamental frequency of the respective data sets. The largest mismatch between the calculated and inferred frequencies for all study sites is 0.016 cycles/pixel (the data from Landsat D′ after the filters were installed). Out of the 85 noise peaks singled out in all the data sets, only 10 have a mismatch of more than ±0.005 cycles/pixel. (The accuracy to which our 4096 point Fourier transform can measure frequency is ±0.003 cycles/pixel.) The match with the observed data is too good to be purely coincidental.

FILTERING LANDSAT-4 MSS COHERENT NOISE

We have devised a technique through which the Landsat-4 MSS coherent noise can be removed with minimal effect to the ground image data. Plate 1b was produced using this technique. We will now describe our technique using the scene in Plate 1 as an example.

The first step is to characterize the coherent noise for the scene in question using the technique dis-

TABLE 11. LANDSAT-4 NORTH CAROLINA DATA INFERRED RELATIONSHIPS AMONG THE FREQUENCIES OF COHERENT NOISE PEAKS IN THE FOURIER MAGNITUDE PLOTS

Observed Frequency (cycles/pixel)	Inferred Harmonic Number	Freq. Inferred from Harmonic (cycles/pixel)	Harmonic × Fund. Freq.* (cycles/pixel)
2.28	2	2.28	2.281
12.46	11	12.54	12.543
10.17	13	14.83	14.824
7.90	15	17.10	17.104
6.76	16	18.24	18.245
5.62	17	19.38	19.385
4.47	18	20.53	20.525
3.33	19	21.67	21.666
2.20	20	22.80	22.806
1.06	21	23.94	23.946
0.09	22	25.09	25.087
1.23	23	26.23	26.227
2.37	24	27.37	27.367
4.64	26	29.64	29.648
5.79	27	30.79	30.788
6.93	28	31.93	31.928
8.07	29	33.07	33.069
9.21	30	34.21	34.209
10.35	31	35.35	35.349
11.49	32	36.49	36.490
12.37	33	37.63	37.630
11.23	34	38.77	38.770
10.09	35	39.91	39.910
9.72	(162)	(184.72)	(184.729)
10.72	(166)	(189.28)	(189.290)
1.28	?	?	?

* Inferred fundamental frequency is 1.1403 cycles/pixel (114.51 kHz). For signal mixing representation, A = 1.1403 cycles/pixel and B = 0.0866 cycles/pixel.

cussed in the Noise Characterization section. This gives us a list of frequency components corresponding to the coherent noise for that scene. The frequency component list for the example scene is given in Table 12.

We next design a zero-one blocking filter based on our noise frequency component list. The blocking filter is set to all ones except in bands surrounding the noise frequency components where the filter is set to zero. The frequency components set to zero in our blocking filter for the example scene are also given in Table 12. The band of frequencies blocked around each noise frequency component is taken to be fairly broad (±2 or 3 cycles/ (4096 samples) from the peak) to allow for rounding the filter to reduce filtering artifacts.

A technique that is often used to round filters is to multiply the filter in the transform domain (here spatial domain) by an elliptical arc (Frieden, 1975). Since our original filter is so sharp (being a 0-1 filter), we increase the rounding effect by using the square of an elliptical arc instead. The 4096 point squared elliptical arc is given by the formula:

$$E(x) = \begin{cases} 1.0 - (((x-1)/2048)^2) & \text{for } 1 \le x \le 2049 \\ 1.0 - (((4097-x)/2048)^2) & \text{for } 2049 < x \le 4096. \end{cases} \quad (4)$$

TABLE 12. FILTER FOR EXAMPLE SCENE (PLATE 1)

Noise Frequency Components		Blocking Filter Zeros
Image Domain Freq. (cycles/pixel)	Sample Domain Freq. (cycles/ (4096 samples))	Sample Domain Freq. (cycles/pixel)
1.23	201	199–203
2.20 and 2.28	360 and 374	357–377
3.33	546	544–548
4.47	733	731–735
5.62	920	918–922
5.79	948	946–951
6.76	1107	1104–1109
6.93	1135	1133–1136
7.90	1294	1291–1296
8.07	1322	1320–1324
9.21	1509	1506–1511
10.35	1696	1692–1698
11.49	1882	1880–1885
12.37	2027	2025–2029
12.46	2041	2039–2043

Note: 25 samples = 1 image domain pixel.

Next we take an inverse Fourier transform of our blocking filter, multiply the result by the elliptical arc squared, and take a forward Fourier transform of the multiplication results. This gives us our rounded blocking filter.

The next step is to filter the chosen section of data. In the example, we filtered a 90 line by 157 column section by starting with a 90 line by 170 column section. For each six-line section (corresponding to the six MSS detectors per band), we resequenced the data into the original sampling sequence (without adding biases to each band) giving 15 separate 1-line by 4099-column resequenced sections. We then took the 4096 point forward Fourier transform of each of these sections, multiplied each by the rounded blocking filter, and took the inverse Fourier transforms. These filtered resequenced sections were then inverse resequenced back into image format. One column of data is effectively lost by taking a Fourier transform of 4096 points rather than 4099 points, and another 12 columns are lost in the inverse resequencing process. Thus a 90-line by 157-column filtered image was produced from an original 90 line by 170 column A-CCT tape image.

As noted earlier, this filtering technique was used to produce the result displayed in Plate 1b. Subtracting the original image from the filtered image gives a difference image which is entirely noise. This difference image (plus a bias) is displayed in Plate 1c. Examining this difference image we can see that the overall coherent noise pattern has a maximum magnitude of plus or minus 3 counts. In the difference image (disregarding the bias), some 58 percent of the pixels have value 0 (i.e., 58 per-

cent of the pixels in the original and filtered images are identical), some 40 percent of the pixels have value ± 1, about 2 percent of the pixels have value ± 2, and less than 0.01 percent of the pixels have value ± 3. The variance of the difference image (in each band) is approximately 0.5.

This evaluation of the total magnitude of the coherent noise effect can only be performed using a technique similar to the one employed here. Other techniques which examine the magnitude of a particular peak in a Fourier transform plot of a portion of the data only give the magnitude of one particular noise frequency. It is not at all clear how one could reliably take some kind of weighted sum of the Fourier magnitude of each noise frequency peak to get the actual overall noise magnitude. The problem would be finding the appropriate weights that would reflect accurately the manner in which each peak constructively or destructively interferes with the other noise peaks. Examining a difference image, such as the one generated by our technique, is the only straightforward way to get a reliable measure of the overall noise magnitude.

CONCLUSIONS

We have analyzed the magnitude of the major Landsat MSS coherent noise component for each detector, and noted the efficacy of the noise reduction filters on the Landsat-5 MSS. In addition, we have described a technique for characterizing the coherent noise by analyzing the data in its original sample order, and have described a companion technique for filtering out the coherent noise. The techniques were demonstrated on Landsat-4 and Landsat-5 MSS data sets (prelaunch and in-flight), and a harmonic explanation of the noise pattern was suggested.

The filtering technique presented in this report can be used to filter out the coherent noise present in the Landsat-4 MSS data already collected. The cleanup of Landsat-4 MSS data would be fairly expensive in terms of computer resources, so we expect that it would only be done for selected high demand scenes. Assuming the RC filters installed by the General Electric Company on the Landsat-D' (prelaunch Landsat-5) continue to perform as well as they have on the data sets we have analyzed, we expect that there will be no need to perform ground based filtering on data produced by Landsat-5.

ACKNOWLEDGMENTS

and performed some of the analysis runs. Dr. Barker provided technical advice and arranged for funding of a large portion of these studies.

REFERENCES

Alford, W. L., and Imhoff, M. L., 1984. Radiometric Accuracy of The Landsat-4 Multispectral Scanner data: in *Landsat-4 Science Investigations Summary*, NASA CP-2326, Vol. II, NASA, Washington, D.C., pp. 69-72.

———— 1985. Radiometric Accuracy of The Landsat-4 Multispectral Scanner data: in *Early Results: Volume I-Multispectral Scanner (MSS)*, NASA CP-2355, NASA, Washington, D.C., pp. I-9 to I-21.

Barker, J. L., ed., 1985. *Landsat-4 Science Characterization Early Results: Volume I-Multispectral Scanner (MSS)*, NASA CP-2355, NASA, Washington, D.C.

Frieden, B. R., 1975. Image Enhancement and Restoration: in *Topics in Applied Physics, Volume 6: Picture Processing and Digital Filtering*, (edited by T.S. Huang), Springer-Verlag, p. 196.

Gordon, F., Jr., 1980. The Time-Space Relationships of the Data Points (Pixels) of the Thematic Mapper and Multispectral Scanner or 'The Myth of Simultaneity': *NASA Technical Paper 1715*, July.

Likens, W. C., and Wrigley, R. C., 1984. Impact of Landsat MSS Sensor Differences on Change Detection Analysis: in *Landsat-4 Science Investigations Summary*, NASA CP-2326, Vol. II, NASA, Washington, D.C., pp. 87-90.

———— 1985. Impact of Landsat MSS Sensor Differences on Change Detection Analysis: in *Early Results: Volume I-Multispectral Scanner (MSS)*, NASA CP-2355, NASA, Washington, D.C., pp. I-159 to I-175.

National Aeronautics and Space Administration, Goddard Space Flight Center, 1984. Landsat To Ground Station Interface Description: *NASA Technical Paper GSFC 436-D-400*, Revision 8, June.

Rice, D. P. and Malila, W. A., 1984. Investigation of Radiometric Properties of Landsat-4 MSS: *Landsat-4 Science Investigations Summary*, NASA CP-2326, Vol. II, NASA, Washington, D.C., pp. 76-80.

———— 1985. Investigation of Radiometric Properties of Landsat-4 MSS: in *Early Results: Volume I-Multispectral Scanner (MSS)*, NASA CP-2355, NASA, Washington, D.C., pp. I-57 to I-75.

Tilton, J. C., Alford, W. L., and Markham, B. L., 1985. Landsat-4 and Landsat-5 MSS Coherent Noise Characterization and Removal: (To be published as a NASA/GSFC Technical Report).

CALL FOR PAPERS

Workshop on Geographic Information Systems

Atlanta, Georgia
1-4 April 1986

This workshop to advance the field of Geographic Information Systems is sponsored by the USDA Forest Service Southern Region and the American Society for Photogrammetry and Remote Sensing. Planned Sessions include

- Training and Awareness
- Applications I
- Data Exchange Formats
- Data Capture and Map Preparation
- Benefit/Cost, Program Administration, Planning, and Budget
- Data Archiving, handling and data bas design
- Applications II
- Modeling with a GIS

Abstracts are due by 15 October, 1985, and Final Manuscripts are due by January 15. Submit Abstracts to

Roy A. Mead
U.S. Forest Service
Room 806
1720 Peachtree Rd., N.W.
Atlanta, GA 30367
Tele. (404) 881-2774